

Accepted Manuscript

IR spectroscopy and chemometrics for physical property prediction of structured lipids produced by interesterification of beef tallow

A. Burcu Aktas, Cristina Alamprese, Dimitrios Fessas, Banu Ozen



PII: S0023-6438(19)30361-5

DOI: <https://doi.org/10.1016/j.lwt.2019.04.057>

Reference: YFSTL 8056

To appear in: *LWT - Food Science and Technology*

Received Date: 31 January 2019

Revised Date: 18 March 2019

Accepted Date: 17 April 2019

Please cite this article as: Aktas, A.B., Alamprese, C., Fessas, D., Ozen, B., IR spectroscopy and chemometrics for physical property prediction of structured lipids produced by interesterification of beef tallow, *LWT - Food Science and Technology* (2019), doi: <https://doi.org/10.1016/j.lwt.2019.04.057>.

This is a PDF file of an unedited manuscript that has been accepted for publication. As a service to our customers we are providing this early version of the manuscript. The manuscript will undergo copyediting, typesetting, and review of the resulting proof before it is published in its final form. Please note that during the production process errors may be discovered which could affect the content, and all legal disclaimers that apply to the journal pertain.

1 **IR spectroscopy and chemometrics for physical property prediction of structured lipids**
2 **produced by interesterification of beef tallow**

3
4 A. Burcu Aktas^{a,b}, Cristina Alamprese^{c*}, Dimitrios Fessas^c, Banu Ozen^b

5
6 ^a Cumhuriyet University, Food Engineering Department, 58140 Sivas, Turkey

7 ^b Izmir Institute of Technology, Food Engineering Department, 35430 Urla-Izmir, Turkey

8 ^c Università degli Studi di Milano, Department of Food, Environmental and Nutritional Sciences
9 (DeFENS), via Celoria 2, 20133 Milan, Italy

10
11 * corresponding author: cristina.alamprese@unimi.it

12
13 Authors' e-mails:

14 A. Burcu Aktas: ayseaktas@iyte.edu.tr

15 Dimitrios Fessas: dimitrios.fessas@unimi.it

16 Banu Ozen: banuozen@iyte.edu.tr

17

18

19 **ABSTRACT**

20 The aim of this study was the application of infrared spectroscopy and chemometrics to predict
21 slip melting point (SMP), melting points at different melted fat percentages (MP85, MP90,
22 MP95), and consistency of structured lipids to provide fast and reliable methods for their
23 characterization. Tallow was chemically or enzymatically interesterified with corn, canola, and
24 safflower oils separately, at different ratios. Fourier-transform mid-infrared (FT-IR) and near-
25 infrared (FT-NIR) spectra of melted and solid samples were collected. Partial-least-square
26 regression models constructed after different spectra pre-treatments and variable selection were
27 satisfactory. The best models were obtained with solid sample FT-NIR spectra: in cross-
28 validation, determination coefficients and root mean square errors were, respectively, 0.85 and
29 1.7 °C for SMP, 0.85 and 2.8 °C for MP90, and 0.91 and 14 MPa for consistency. Infrared
30 spectroscopy can be considered a promising tool to determine physical properties of
31 interesterified fats.

32
33 *Keywords:* calorimetry; chemometrics; consistency; infrared spectroscopy; slip melting point.

34

35 **1. Introduction**

36 Beef tallow is considered as a low-value fat since it is not suitable for direct human consumption
37 due to its high melting point, wide plastic range, and low levels of polyunsaturated fatty acids
38 (Kowalska, Żbikowska, & Kowalski, 2004). Therefore, physical properties of tallow need to be
39 modified to enhance its value and potential uses. Modifications can be achieved by either
40 chemical or enzymatic interesterification (Engelmann et al., 2018). Chemical interesterification
41 provides new physical properties to the modified lipids by the random incorporation or the
42 restructuring of acyl residues of triacylglycerols (TAG). On the contrary, enzymatic
43 interesterification leads to the attachment of specific fatty acids to specific positions of TAG
44 structure to produce new products (Martin, Reglero, & Señoráns, 2010). One of the goals of
45 interesterification processes is to modify fat consistency, which is an important quality aspect,
46 usually defined as spreadability and hardness (De Graef, Vereecken, Smith, Bhagga, &
47 Dewettinck, 2012).

48 Tallow is hard at ambient temperature, thus its use in several food products is limited. High
49 melting and slip melting points (about 40-60 °C) are other handicaps that prevent the direct use of
50 tallow in foods. Thus, for use in edible products, tallow should be modified to obtain fats with
51 desirable properties (Bhattacharyya, Bhattacharyya, & De, 2000).

52 Infrared (IR) spectroscopy is a promising technique for the analyses of fats and oils, with the
53 advantages of being fast, non-destructive, and easy-to-use; moreover, minimum or no sample
54 preparation is required before analysis. In the scientific literature, there are many examples of IR
55 spectroscopy applications to determine fat and oil properties (Cascañt et al., 2018; Gertz &
56 Behmer, 2014; Hocevar, Soares, Oliveira, Korn, & Teixeira, 2012; Özdemir et al., 2018). For
57 instance, in a study about the direct characterization of lard (i.e., without performing sample
58 pretreatment steps like melting or homogenization) by means of Fourier-transform near-infrared

59 (FT-NIR) spectroscopy, the results of the multivariate model calibration showed that the
60 selection of the most relevant wavelengths enables the accurate prediction of iodine number and
61 fatty acid profile (Foca et al., 2016). The suitability of IR spectroscopy in monitoring lipase-
62 catalyzed interesterification of bulky fats was also demonstrated (Chang, Lai, Zhang,
63 S ndergaard, & Xu, 2005). Mid-IR spectroscopy in combination with chemometric techniques
64 such as partial least square regression was successfully employed for the determination of the
65 composition of waste frying oils consisting of soybean oil, palm oil, and hydrogenated vegetable
66 fat (Hocevar et al., 2012). In another study, the possibility of monitoring hydrogenation process
67 of soybean oil by a compact near-IR spectrometer and the suitable data elaboration was
68 demonstrated (Pereira et al., 2018).

69 However, to the best of our knowledge, no studies regarding the prediction of physical
70 parameters of interesterified products using IR spectroscopy have been published. The hypothesis
71 of this research is that IR spectroscopy, coupled to chemometrics, is able to characterize physical
72 properties of structured fats obtained by interesterification. Actually, interesterification reactions
73 modify fat physical features by TAG rearrangement. The exchange of acyl groups among TAG
74 leads to changes in molecular vibrations that can be detected by IR spectroscopy. The aim of this
75 study was, therefore, to investigate the capability of FT-NIR and Fourier-transform mid-infrared
76 (FT-IR) spectroscopy to predict some physical properties (consistency, slip melting point, and
77 melting point) of structured lipids produced by chemical and enzymatic interesterification of
78 tallow with different ratios of canola, corn, or safflower oils.

79

80 **2. Materials and methods**

81 *2.1. Production of interesterified lipids*

82 The tallow used for interesterification reactions was obtained from two different breeds
83 (Montafon and Holstein) of 2-years old calves immediately after slaughter. Canola, corn, and
84 safflower oils were obtained from local market. Calf breed and oil type were not considered as
85 experimental variables. Sodium methoxide was provided by a local oil processing plant. Lipase
86 solution from *Thermomyces lanuginosus* was purchased from Sigma–Aldrich (St. Louis, MO).
87 Sixty different structured lipids were manufactured by chemical and enzymatic interesterification
88 following published procedures (Bryś, Wirkowska, Górska, Ostrowska-Ligeza, & Bryś, 2014;
89 Kowalska et al., 2014). All structured lipids were prepared at three different tallow/oil blend
90 ratios (6:4, 7:3, and 8:2 w/w). Chemically interesterified lipids were produced by adding the
91 catalyst at different concentrations (0.75, 0.875 or 1 g/100 g). For the manufacturing of
92 enzymatically interesterified lipids, the reaction was achieved by adding 10 g/100 g enzyme.
93 After production, all structured fats were stored at -20 °C until analyses.

94

95 2.2. Determination of slip melting and melting points

96 Slip melting point (SMP) of structured fats, non-interesterified blends, and tallow was determined
97 according to AOCS method Cc 3-25 (AOCS, 1989). Samples were heated to 60 °C in a
98 thermostatic chamber for complete melting of the crystals. Capillary tubes filled with melted
99 samples were chilled at 4 °C overnight before being immersed in a beaker of distilled water at
100 ambient temperature. The water was heated at a rate of 1.2 K/min and the temperature at which
101 the column of fat rose in the tube was recorded as SMP. This measurement was carried out at
102 least twice for each sample.

103 Melting point of structured lipids, non-interesterified blend, and tallow was measured by
104 differential scanning calorimetry (DSC) using a Q10 calorimeter (TA Instruments, Crawley, UK).

105 Samples (9-10 mg) were placed in hermetically sealed aluminum pans. DSC analysis was carried
106 out from 20 to -40 °C and from -40 to 80 °C at a scan rate of 10 K/min compared to an empty pan
107 (Rodríguez, Castro, Salinas, López, & Miranda, 2001). Data analysis was performed with the
108 dedicated software IFESTOS which was assembled by some of the Authors for handling raw
109 calorimetric data according to the suggestions of Barone, Del Vecchio, Fessas, Giancola, and
110 Graziano (1993). Briefly, the output signal in mW units was divided by the product of sample
111 mass and heating rate to be converted into apparent specific heat and it was scaled with respect to
112 the baseline to obtain the excess (with respect to the melted state) specific heat trace, C_p^{exc}
113 [J/(K·g)]. Thanks to this treatment, the area beneath the recorded peaks directly corresponds to
114 the relevant transition enthalpy, $\Delta H_{overall}$. Accordingly, the degree of the overall melting process
115 as a function of temperature, $\alpha(T)$ (ranging from 0 to 1), was obtained by the following equation:

$$116 \quad \alpha(T) = \frac{\int_{T_0}^T C_p^{exc} dT}{\Delta H_{overall}} \quad [\text{Eq. 1}].$$

117 i.e., the ratio of the partial area at a given temperature to the overall area of the DSC peaks was
118 used to obtain the percentage of the melted material in the sample at each temperature.

119

120 2.3. Consistency measurements

121 Structured lipids and tallow samples (5 g) were put into 10 mL glass beakers and heated to 60 °C
122 in a thermostatic chamber for complete melting. Then, they were conditioned for 24 h in another
123 thermostatic chamber at 25 °C. Consistency of samples was determined by penetration tests
124 carried out using a 45° acrylic cone fitted to a TA.XT Plus texture analyzer (Stable Micro
125 Systems, Surrey, UK). A penetration depth of 4 mm with a 20 mm/s speed was applied, and
126 consistency was calculated as “yield value” according to the following equation (Silva et al.,
127 2009):

$$C = \frac{KW}{p^{1.6}} \quad [\text{Eq. 2}]$$

128 where C is the yield value (MPa), K is a constant depending on the cone angle (4700
129 adimensional), W is the compression force (N), and p is the penetration depth (m). Measurements
130 were performed in triplicate.
131

132

133 2.4. FT-NIR spectroscopy analyses

134 FT-NIR spectra were acquired with a MPA spectrometer (Bruker Optics, Milan, Italy) on both
135 melted and solid structured lipids as well as on tallow, and non-interesterified blends. After
136 melting in a temperature-controlled chamber at 60 °C for 2 h, the samples (50 mL) were
137 transferred in a water bath at 60 °C and FT-NIR spectra were acquired in transreflectance mode (1
138 mm pathlength) by a fiber optic reflection probe (1.5 m length) inserted directly in the lipid. A
139 spectral range of 12500-3600/cm was used, with 8/cm resolution, and 32 scans for both
140 background and samples. For measurements on solid samples, melted lipids were poured in
141 disposable glass vials (8 mm pathlength) and incubated overnight at 25 °C in a temperature-
142 controlled chamber. FT-NIR spectra were then collected in transmission mode by using the same
143 analytical conditions applied for the melted samples. All spectra were acquired in duplicate and
144 the instrument control was performed by OPUS software (v. 6.5 Bruker Optics, Ettlingen,
145 Germany).

146

147 2.5. FT-IR spectroscopy analyses

148 FT-IR spectra were acquired with a Vertex 70 spectrometer (Bruker Optics, Milan, Italy)
149 controlled by OPUS software (v. 6.5 Bruker Optics, Ettlingen, Germany) on both melted and
150 solid structured lipids as well as on tallow, and non-interesterified blends. Spectra were collected

151 over the range of 4000-700/cm, at 4/cm resolution, by using a single reflection ZnSe ATR cell
152 (MIRacle™, PIKE Technologies, Inc., Madison, WI) and 32 scans for both samples and
153 background. Measurements were replicated twice on samples prepared as already reported for
154 FT-NIR analyses. Melted samples were poured on the ATR cell by means of a pipette, while
155 solid fats were spread on the ATR crystal by means of a spatula.

156

157 2.6. Data analysis

158 FT-IR and FT-NIR data are complex so, to extract useful information, multivariate analysis
159 techniques were applied by means of The Unscrambler X software (v. 10.4.1, CAMO Process
160 A/S, Oslo, Norway). Four data matrices with 71 samples including tallow (2), interesterified
161 lipids (60), and non-interesterified blends (9) were constructed with FT-NIR and FT-IR spectra of
162 both melted and solid samples. The following wavenumber ranges were selected in order to keep
163 the most informative and less noisy segments of the spectra:

- 164 - FT-NIR: 9002-4497/cm
- 165 - FT-IR: 3051-2599 and 2052-597/cm.

166 For all matrices, the replicated spectra were averaged prior to the application of various pre-
167 processing techniques including smoothing (moving average, segment size: 7), standard normal
168 variate (SNV), multiplicative scatter correction (MSC), first (d1) and second (d2) derivatives
169 (Savitzky-Golay, 11 smoothing points). The partial least square regression (PLS) analysis was
170 applied to each pre-treated data matrices in order to predict the physical properties of
171 interesterified lipids. Due to the limited number of samples, models were validated only by an
172 internal cross-validation procedure, considering 5 randomly created cancellation groups. The best
173 models were selected based on the following figures of merit: determination coefficient (R^2), root
174 mean square error of calibration (RMSEC) and cross-validation (RMSECV), number of latent

175 variables (LVs). Variable selection was carried out by the Martens uncertainty test implemented
176 in The Unscrambler X.

177 A Pearson correlation matrix for SMP and melting points at the different percentages of melted
178 fat was calculated (Statgraphics Centurion 18, Statgraphics Technologies Inc., The Plains, VA,
179 USA).

180

181 **3. Results and discussion**

182 *3.1. Physical properties of structured lipids*

183 SMP of structured lipids ranged from 31.8 to 47.1 °C as reported in Table 1. Interesterification
184 reactions, as expected, caused a decline in SMP of structured lipids in comparison to the tallow
185 and the non-interesterified blends, due to the changes in TAG composition caused by the
186 reactions (Oliveira et al., 2017).

187 The detailed picture of the melting behavior of structured lipids was obtained by DSC, which
188 provides useful information about the crystal thermal stability of interesterified fats. As an
189 example, in Fig. 1 the DSC melting profile of a chemically interesterified sample of a canola-
190 tallow blend is shown. A complex endothermic trace can be observed, with at least three main
191 endothermic peaks with shoulders, across a wide temperature range, corresponding to the melting
192 of different TAG crystals. Actually, in the present work tallow was interesterified with different
193 vegetables oils, therefore different TAGs were created in the structured lipid throughout the
194 reaction. The overall inspection of the DSC measurements suggests that the low temperature
195 melting peak (Peak 1) is associated with TAGs of vegetable oils, i.e. can be attributed to the
196 presence of a high content of mono- and poly-unsaturated fatty acids. Peak 2 represents middle-
197 melting TAG species, naturally present in non-interesterified blends and/or formed during
198 interesterification. Peak 3 represents the high-melting species associated with saturated TAGs

199 deriving from tallow. In this complex scenario, i.e. a mixture of crystals with different thermal
200 stability, it is difficult to define a sample specific melting point to find a correlation with the
201 SMP. For this reason, the integral form of the DSC traces was taken into account (Fig. 1), i.e. the
202 overall degree of the advance of melting process as a function of temperature ($\alpha(T)$), and melting
203 points as a function of given percentages of melted crystals (85, 90, and 95%) were calculated
204 (MP85, MP90, and MP95; Table 1). In all cases, as already observed for SMP, interesterification
205 reactions caused a decrease in the melting points of structured lipids compared to tallow and the
206 non-interesterified blends. These changes in melting points are in accordance with previous
207 studies (Li et al., 2018; Morselli Ribeiro, Ming, Silvestre, Grimaldi, & Gonçalves, 2017;
208 Wirkowska-Wojdyla, Brys, Górska, & Ostrowska-Ligeza, 2016). As regards the melting
209 percentage that better correlates melting point with SMP, highly significant ($p < 0.001$) Pearson
210 correlations were found between SMP and all the determined melting points. However, the
211 correlation between SMP and MP95 ($r = 0.892$; Fig. 2) was considered the best one, since the
212 lower bias was obtained (8.7 °C vs 30.0 and 18.9 °C for MP85 and MP90, respectively). In any
213 case, it has to be noticed that the DSC temperature scan rate was higher than that of the SMP
214 method and this difference may generate, in some cases, further uncertainty.

215 Consistency of the samples was calculated as “yield value” (MPa) and the obtained ranges are
216 listed in Table 1. As expected, the consistency of tallow was quite higher than both interesterified
217 lipids and non-interesterified blends. Therefore, consistency of blends increased with the
218 increasing amount of tallow. Interesterified lipids tended to show lower consistency values
219 compared to their corresponding blends before the reactions, probably due to higher amounts of
220 tri-unsaturated TAGs produced by interesterification. In addition, differences in polymorphic

221 structure and aggregation behavior, which lead to alteration in the structure of tallow crystal
222 network, can change the consistency (Silva et al., 2009).

223

224 *3.2. IR spectral profiles of structured lipids*

225 The reduced (without non-informative wavenumber regions) FT-NIR and FT-IR spectra of
226 melted and solid interesterified lipids and non-interesterified blends are shown in Fig. 3. In FT-
227 NIR spectra, absorption bands between 6055 and 5345/cm appeared to be highly significant. This
228 region is mainly related to the first overtone of C-H stretching in fatty acid molecules (Blanco et
229 al., 2004). Despite the high values of absorbance observed in both melted and solid samples,
230 signal saturation was not reached, while it appeared in the discarded spectral region (i.e. 4497-
231 3600/cm). The absorption peak in the 5345-4562/cm region is ascribable to the combination band
232 of O-H and C=O stretching of ester groups (RCOOR). The region 7397-6661/cm corresponds to
233 the first overtone of the O-H bond of mono- and diglycerides that might be produced as
234 intermediates and by-products during interesterification reactions (Blanco, Beneyto, Castillo, &
235 Porcel, 2004; Chang et al., 2005). FT-NIR spectra of solid samples showed higher absorbance
236 values and baseline trend in comparison to melted samples, probably due to scattering effects
237 caused by the fat crystals (Chang et al., 2005) and to the longer pathlength used (8 mm vs 1 mm).
238 For all FT-IR spectra, more attention was paid to the fingerprint region (1500-800/cm). This
239 region includes C-O-C vibration in esters, C-H bending and stretching vibrations, and the second
240 overtone of C=O and -OH in fatty acid structure (Chang et al., 2005; Moh, Tang, Man, & Lai,
241 1999). Melted and solid sample spectra were more similar than in the case of FT-NIR region,
242 because scattering effects are less important in FT-IR region (Doyle, 1995). Moreover, the very
243 little amount of sample used for FT-IR spectra collection and the absence of a temperature

244 control, made melted samples partially solidify during measurements, thus decreasing differences
245 with respect to previously crystallized samples.

246

247 *3.3. Prediction of physical parameters from infrared spectra with partial least square analysis*

248 The capability of predicting melting properties and consistency of interesterified fats from IR
249 spectra was investigated by constructing PLS models. All regression models were developed
250 using both FT-NIR and FT-IR spectra of solid and melted samples individually. The detailed PLS
251 results are shown in Tables 2 and 3 in terms of number of LVs, coefficients of determination in
252 calibration (R^2_{cal}) and cross-validation (R^2_{cv}), RMSEC and RMSECV. For each response
253 variable, the best models (reported in bold in Tables 2 and 3) were chosen based on lower
254 number of LVs, higher R^2 , and lower errors. In general, the regression models were characterized
255 by a low number of LVs (from 4 to 10) and limited errors compared to the values of the response.
256 Better results were usually obtained using FT-NIR data of solid samples. Even if during FT-IR
257 analyses of melted samples a partial solidification could occur due to the lack of temperature
258 control, models calculated with spectral data of melted samples were similar to or even better
259 than those based on data of solid samples. Actually, as already commented, scattering effects are
260 less important in FT-IR, making composition of samples more important than their state for
261 physical properties prediction.

262 The best PLS model for SMP was obtained with the FT-NIR spectra of solid samples after first
263 derivative transformation. The limited errors and the high determination coefficients prove that it
264 is possible to predict SMP of structured lipids by means of FT-NIR spectroscopy.

265 All the models constructed for the prediction of melting points based on FT-NIR spectra were
266 satisfactory. On the contrary, FT-IR models calculated using solid sample data showed lower R^2_{cv}
267 (0.58-0.67) and higher RMSECV (3.6-5.1 °C), thus being not satisfactory. The lower

268 performances of these models can be due to the very limited amount of sample used for spectra
269 acquisition, possibly not representing the real structure of crystallized lipids. Actually, the best
270 models for melting point prediction were calculated using FT-NIR spectra of solid samples
271 acquired in transmission mode. In this case, a higher amount of sample compared to FT-IR
272 analysis was used, being thus more representative of the whole fat.

273 Similarly, only FT-NIR spectra collected on solid samples provided good prediction models for
274 consistency. In particular, the model based on MSC pre-treated data provided high determination
275 coefficients (0.94 and 0.86 in calibration and cross-validation, respectively) with RMSEC and
276 RMSECV of 11.9 and 18.3 MPa, respectively.

277 The best models were also re-calculated using only the wavenumbers selected by the Martens
278 uncertainty test, in order to obtain simpler and more robust models (Table 4). This procedure did
279 not allow choosing a very limited number of variables, but, in any case, a significant reduction
280 was obtained. Indeed, the number of FT-NIR selected variables was 1169 and 1168 respectively
281 for melted and solid sample (vs a total of 4505 wavenumbers), while 496 and 488 variables were
282 chosen from FT-IR spectra of melted and solid samples, respectively (vs a total of 1907
283 wavenumbers). The construction of PLS models using the selected variables provided a general
284 slight improvement in prediction ability of the models, lowering the number of LVs, reducing
285 RMSECV and increasing R^2_{cv} . The best improvement was obtained for consistency prediction.

286 The best performances of FT-NIR spectroscopy applied to solid samples were confirmed.

287 There is limited information in the literature regarding the estimation of lipid physical properties
288 by using IR spectroscopy. However, the results of this research are in agreement with a study
289 about the monitoring of lipase-catalyzed interesterification of vegetable fats (Chang et al., 2005).

290 The authors demonstrated that FT-NIR analysis of the interesterified products in solid form

291 exhibited higher correlations with conventional methods with respect to FT-NIR spectroscopy
292 applied to liquid samples or FT-IR spectroscopy of both solid and melted fats.

293

294 **4. Conclusions**

295 In this study, the application of FT-NIR and FT-IR spectroscopy for the prediction of SMP, MP,
296 and consistency of various interesterified lipids was investigated. The use of PLS regression
297 analysis coupled with different spectral data pre-treatments provided satisfactory models for the
298 predictions of the physical properties, thus confirming the formulated hypothesis. The work
299 represents a proof of concept that IR spectroscopy can be used for structured fat characterization,
300 thus providing producers with rapid and non-destructive techniques as good alternatives to the
301 traditional analytical methods.

302 Future developments should be focused on the collection of a higher number of FT-NIR spectra
303 of liquid samples at different interesterification stages, in order to improve the developed models
304 and propose in-line applications for industrial processing.

305

306 **Acknowledgements**

307 We would like to thank the Geothermal Energy Research and Application Center Izmir Institute
308 of technology (Izmir, Turkey) for helping in DSC measurements.

309

310 **Funding**

311 This study was financially supported by Izmir Institute of Technology Scientific Research
312 Projects (IYTE SRP) Program (Project No: 2017-IYTE-3).

313

314 **Conflicts of interest**

315 Declarations of interest: none

316

317 **References**

318 AOCS (1989). Method Cc 3-25. Slip Melting Point, AOCS Standard Open Tube Melting Point.

319 In *Official Methods and Recommended Practices of the AOCS* (3rd ed.). Champaign: The

320 American Oil Chemists' Society.

321 Barone, G., Del Vecchio, P., Fessas, D., Giancola, C., Graziano, G. (1993). The deconvolution of
322 multistate transition DSC curves of biological macromolecules: bovine serum albumin and
323 bovine seminal ribonuclease. *Thermochimica Acta*, 227, 185-195.

324 Bhattacharyya, S., Bhattacharyya, D. K., & De, B. K. (2000). Modification of tallow fractions in
325 the preparation of edible fat products. *European Journal of Lipid Science and Technology*,
326 102, 323-328.

327 Blanco, M., Beneyto, R., Castillo, M., & Porcel, M. (2004). Analytical control of an esterification
328 batch reaction between glycerine and fatty acids by near-infrared spectroscopy. *Analytica*
329 *Chimica Acta*, 521, 143-148.

330 Bryś, J., Wirkowska, M., Górka, A., Ostrowska-Liżęza, E., & Bryś, A. (2014). Application of
331 the calorimetric and spectroscopic methods in analytical evaluation of the human milk fat
332 substitutes. *Journal of Thermal Analysis and Calorimetry*, 118, 841-848.

333 Cascant, M. M., Breil, C., Fabiano-Tixier, A. S., Chemat, F., Garrigues, S., & de la Guardia, M.
334 (2018). Determination of fatty acids and lipid classes in salmon oil by near infrared
335 spectroscopy. *Food Chemistry*, 239, 865-871.

336 Chang, T., Lai, X., Zhang, H., Søndergaard, I., & Xu, X. (2005). Monitoring lipase-catalyzed
337 interesterification for bulky fat modification with FT-IR/NIR spectroscopy. *Journal of*
338 *Agricultural and Food Chemistry*, 53, 9841-9847.

- 339 De Graef, V., Vereecken, J., Smith, K. W., Bhaggan, K., & Dewettinck, K. (2012). Effect of TAG
340 composition on the solid fat content profile, microstructure, and hardness of model fat
341 blends with identical saturated fatty acid content. *European Journal of Lipid Science and*
342 *Technology*, 114, 592-601.
- 343 Doyle, W. M. (1995). Near-IR and mid-IR process analysis-a critical comparison. *Advances in*
344 *Instrumentation and Control*, 50, 433-441.
- 345 Engelmann, J. I., Silva, P. P., Igansi, A. V., Pohndorf, R. S., Cadaval Jr, T. R. S., Crexi, V. T., &
346 Pinto, L. A. A. (2018). Structured lipids by swine lard interesterification with oil and esters
347 from common carp viscera. *Journal of Food Process Engineering*, 41, e12679.
- 348 Foca, G., Ferrari, C., Ulrici, A., Ielo, M. C., Minelli, G., & Fiego, D. P. L. (2016). Iodine value
349 and fatty acids determination on pig fat samples by FT-NIR spectroscopy: benefits of
350 variable selection in the perspective of industrial applications. *Food Analytical Methods*, 9,
351 2791-2806.
- 352 Gertz, C., & Behmer, D. (2014). Application of FT-NIR spectroscopy in assessment of used
353 frying fats and oils. *European Journal of Lipid Science and Technology*, 116, 756-762.
- 354 Hocevar, L., Soares, V. R., Oliveira, F. S., Korn, M. G. A., & Teixeira, L. S. (2012). Application
355 of multivariate analysis in mid-infrared spectroscopy as a tool for the evaluation of waste
356 frying oil blends. *Journal of the American Oil Chemists' Society*, 89, 781-786.
- 357 Kowalska, M., Zbikowska, A., & Kowalski, B. (2014). Enzymatically modified fats based on
358 mutton tallow and rapeseed oil suitable for fatty emulsions. *Journal of the American Oil*
359 *Chemists' Society*, 91, 1703-1710.
- 360 Li, Y., Zhao, J., Xie, X., Zhang, Z., Zhang, N., & Wang, Y. (2018). A low trans margarine fat
361 analog to beef tallow for healthier formulations: Optimization of enzymatic

- 362 interesterification using soybean oil and fully hydrogenated palm oil. *Food Chemistry*,
363 255, 405-413.
- 364 Martin, D., Reglero, G., & Señoráns, F. J. (2010). Oxidative stability of structured lipids.
365 *European Food Research and Technology*, 231, 635-653.
- 366 Moh, M. H., Tang, T. S., Man, Y. C., & Lai, O. M. (1999). Rapid determination of peroxide
367 value in crude palm oil products using Fourier transform infrared spectroscopy. *Journal*
368 *of Food Lipids*, 6, 261-270.
- 369 Morselli Ribeiro, M. D., Ming, C. C., Silvestre, I. M., Grimaldi, R., & Gonçalves, L. Ap. G.
370 (2017). Comparison between enzymatic and chemical interesterification of high oleic
371 sunflower oil and fully hydrogenated soybean oil. *European Journal of Lipid Science and*
372 *Technology*, 119, 1500473.
- 373 Oliveira, P. D., Rodrigues, A. M., Bezerra, C. V., & Silva, L. H. (2017). Chemical
374 interesterification of blends with palm stearin and patawa oil. *Food Chemistry*, 215, 369-
375 376.
- 376 Özdemir, İ. S., Dağ, Ç., Özinanç, G., Suçsoran, Ö., Ertaş, E., & Bekiroğlu, S. (2018).
377 Quantification of sterols and fatty acids of extra virgin olive oils by FT-NIR spectroscopy
378 and multivariate statistical analyses. *LWT-Food Science and Technology*, 91, 125-132.
- 379 Pereira, J. M. G., Sanchez, J. L., de Lima, P. C., Possebon, G., Tanamati, A., Tanamati, A. A. C.,
380 & Bona, E. (2018). Industrial hydrogenation process monitoring using ultra-compact Near-
381 Infrared Spectrometer and chemometrics. *Food Analytical Methods*, 11, 188-200.
- 382 Rodríguez, A., Castro, E., Salinas, M. C., López, R., & Miranda, M. (2001). Interesterification of
383 tallow and sunflower oil. *Journal of the American Oil Chemists' Society*, 78, 431-436.
- 384 Silva, R. C., Cotting, L. N., Poltronieri, T. P., Balcão, V. M., de Almeida, D. B., Goncalves, L.
385 A., ... & Gioielli, L. A. (2009). The effects of enzymatic interesterification on the physical-

386 chemical properties of blends of lard and soybean oil. *LWT-Food Science and Technology*,
387 42, 1275-1282.

388 Wirkowska-Wojdyla, M., Bryś, J., Górska, A., & Ostrowska-Ligęza, E. (2016). Effect of
389 enzymatic interesterification on physiochemical and thermal properties of fat used in
390 cookies. *LWT-Food Science and Technology*, 74, 99-105.

391

ACCEPTED MANUSCRIPT

392 **Legends to Figures**

393 **Fig. 1.** Differential Scanning Calorimetry melting profile of a chemically interesterified sample
394 of canola-tallow blend.

395
396 **Fig. 2.** Correlation between slip melting point (SMP) and melting point at 95% melted fat
397 (MP95) of structured lipids produced by chemical or enzymatic interesterification of tallow with
398 different vegetable oils.

399
400 **Fig. 3.** Reduced spectra of structured lipids produced by chemical or enzymatic interesterification
401 of tallow with different vegetable oils: a) FT-NIR spectra of melted samples; b) FT-NIR spectra
402 of solid samples; c) FT-IR spectra of melted samples; d) FT-IR spectra of solid samples.

Table 1. Minimum-maximum ranges and standard deviation (s.d.) values of physical properties for structured lipids (60 samples) produced by chemical or enzymatic interesterification of tallow with different vegetable oils. Data for tallow (2 samples) and non-interesterified blends (9 samples) are also reported.

| Response | Structured lipids (min-max value) | Tallow (min-max value) | Non-interesterified blends (min-max value) |
|-------------------|--------------------------------------|---------------------------|---|
| SMP (°C) | 31.8-47.1 | 47.0-50.4 | 43.2-47.1 |
| MP85 (°C) | 18.2-50.0 | 46.6-52.1 | 38.9-50.0 |
| MP90 (°C) | 28.7-50.8 | 48.0-52.8 | 40.1-50.8 |
| MP95 (°C) | 30.2-51.9 | 49.6-53.7 | 40.7-51.9 |
| Consistency (MPa) | 1.5-293.4 | 69.9-603 | 9.0-67.6 |

Table 2.

Statistical parameters of developed PLS models for the prediction of melting and consistency properties of structured lipids by FT-NIR data acquired both on melted and solid samples. The best models are reported in bold.

| Response | Melted samples | | | | | | Solid samples | | | | | |
|-------------------|----------------|-----------|-------------|-------------|-------------|-------------|---------------|-----------------------|-------------|-------------|-------------|-------------|
| | Pretreatment | LVs | RMSEC | R^2_{cal} | RMSECV | R^2_{cv} | Pretreatment | LVs | RMSEC | R^2_{cal} | RMSECV | R^2_{cv} |
| SMP (°C) | SNV | 10 | 1.6 | 0.86 | 2.3 | 0.72 | SNV | 7 | 1.6 | 0.86 | 2.0 | 0.80 |
| | MSC | 10 | 1.6 | 0.86 | 2.4 | 0.72 | MSC | 7 | 1.7 | 0.85 | 2.1 | 0.78 |
| | d1 | 6 | 2.0 | 0.79 | 2.6 | 0.68 | d1 | 5 | 1.3 | 0.91 | 1.6 | 0.88 |
| | d2 | 10 | 1.4 | 0.90 | 2.1 | 0.78 | d2 | 3 | 1.9 | 0.82 | 2.0 | 0.80 |
| MP85 (°C) | SNV | 9 | 3.8 | 0.78 | 4.9 | 0.63 | SNV | 9 | 2.5 | 0.90 | 3.4 | 0.83 |
| | MSC | 9 | 3.8 | 0.77 | 4.9 | 0.65 | MSC | 8 | 2.3 | 0.86 | 3.7 | 0.79 |
| | d1 | 6 | 4.3 | 0.71 | 5.4 | 0.55 | d1 | 6 | 2.7 | 0.88 | 3.4 | 0.83 |
| | d2 | 10 | 2.6 | 0.89 | 3.7 | 0.76 | d2 | 6 | 2.8 | 0.88 | 3.8 | 0.80 |
| MP90 (°C) | SNV | 10 | 2.8 | 0.84 | 4.2 | 0.64 | SNV | 8 | 2.4 | 0.89 | 3.3 | 0.81 |
| | MSC | 10 | 2.8 | 0.84 | 3.9 | 0.69 | MSC | 10 | 2.1 | 0.91 | 3.0 | 0.83 |
| | d1 | 6 | 3.6 | 0.74 | 4.6 | 0.59 | d1 | 6 | 2.4 | 0.89 | 2.8 | 0.84 |
| | d2 | 9 | 2.5 | 0.87 | 3.4 | 0.78 | d2 | 4 | 2.8 | 0.84 | 3.5 | 0.78 |
| MP95 (°C) | SNV | 10 | 2.4 | 0.85 | 3.4 | 0.73 | SNV | 10 | 2.0 | 0.90 | 2.7 | 0.84 |
| | MSC | 9 | 2.8 | 0.8 | 3.6 | 0.68 | MSC | 8 | 2.4 | 0.85 | 3.0 | 0.79 |
| | d1 | 10 | 2.4 | 0.85 | 3.2 | 0.74 | d1 | 6 | 2.3 | 0.86 | 2.9 | 0.78 |
| | d2 | 10 | 2.5 | 0.84 | 3.4 | 0.71 | d2 | 7 | 2.2 | 0.88 | 2.9 | 0.79 |
| Consistency (MPa) | SNV | 10 | 17.2 | 0.87 | 40.7 | 0.25 | SNV | No significant models | | | | |
| | MSC | 7 | 17.2 | 0.87 | 38.9 | 0.35 | MSC | 7 | 11.9 | 0.94 | 18.3 | 0.86 |
| | d1 | 4 | 14.3 | 0.81 | 24.6 | 0.41 | d1 | 10 | 10.4 | 0.95 | 25.6 | 0.68 |
| | d2 | 4 | 16.3 | 0.88 | 36.3 | 0.44 | d2 | 1 | 32.5 | 0.53 | 36.9 | 0.40 |

SMP, slip melting point; MP85, melting point at 85% melted crystals; MP90, melting point at 90% melted crystals; MP95, melting point at 95% melted crystals; SNV, Standard Normal Variate; MSC, Multiplicative Scatter Correction; d1, first derivative; d2, second derivative; LVs, latent variables; RMSEC, root mean square error of calibration; R^2_{cal} , determination coefficient of calibration; RMSECV, root mean square error of cross-validation; R^2_{cv} , determination coefficient of cross-validation.

Table 3. Statistical parameters of developed PLS models for the prediction of melting and consistency properties of structured lipids by FT-IR data acquired both on melted and solid samples. The best models are reported in bold.

| Response | Melted samples | | | | | | Solid samples | | | | | |
|-------------------|----------------|----------|------------|-------------|------------|-------------|---------------|-----------|------------|-------------|------------|-------------|
| | Pretreatment | LVs | RMSEC | R^2_{cal} | RMSECV | R^2_{cv} | Pretreatment | LVs | RMSEC | R^2_{cal} | RMSECV | R^2_{cv} |
| SMP (°C) | SNV | 8 | 1.7 | 0.85 | 2.5 | 0.70 | SNV | 5 | 2.7 | 0.63 | 3.3 | 0.47 |
| | MSC | 7 | 1.8 | 0.83 | 2.6 | 0.66 | MSC | 5 | 2.7 | 0.61 | 3.3 | 0.50 |
| | d1 | 6 | 1.7 | 0.84 | 2.3 | 0.73 | d1 | 7 | 1.8 | 0.83 | 2.5 | 0.68 |
| | d2 | 5 | 1.8 | 0.83 | 2.2 | 0.75 | d2 | 9 | 1.4 | 0.90 | 2.4 | 0.70 |
| MP85 (°C) | SNV | 9 | 3.1 | 0.85 | 5.0 | 0.59 | SNV | 5 | 5.3 | 0.55 | 6.2 | 0.41 |
| | MSC | 7 | 3.6 | 0.80 | 4.8 | 0.65 | MSC | 5 | 5.4 | 0.54 | 6.3 | 0.35 |
| | d1 | 6 | 3.4 | 0.82 | 4.6 | 0.68 | d1 | 10 | 3.0 | 0.85 | 5.1 | 0.58 |
| | d2 | 5 | 3.7 | 0.78 | 4.5 | 0.70 | d2 | 5 | 4.4 | 0.70 | 5.2 | 0.56 |
| MP90 (°C) | SNV | 9 | 2.6 | 0.86 | 4.3 | 0.65 | SNV | 5 | 4.4 | 0.61 | 5.2 | 0.45 |
| | MSC | 7 | 3.0 | 0.82 | 4.0 | 0.69 | MSC | 5 | 4.4 | 0.60 | 5.1 | 0.49 |
| | d1 | 6 | 2.9 | 0.83 | 3.9 | 0.70 | d1 | 9 | 2.7 | 0.85 | 4.6 | 0.60 |
| | d2 | 4 | 3.3 | 0.78 | 3.9 | 0.71 | d2 | 5 | 3.7 | 0.72 | 4.5 | 0.60 |
| MP95 (°C) | SNV | 8 | 2.3 | 0.86 | 3.4 | 0.71 | SNV | 5 | 3.7 | 0.65 | 4.5 | 0.51 |
| | MSC | 7 | 2.4 | 0.85 | 3.3 | 0.71 | MSC | 5 | 3.7 | 0.65 | 4.5 | 0.49 |
| | d1 | 3 | 3.1 | 0.75 | 3.4 | 0.71 | d1 | 10 | 2.1 | 0.88 | 3.6 | 0.67 |
| | d2 | 4 | 2.9 | 0.79 | 3.4 | 0.72 | d2 | 4 | 3.5 | 0.68 | 3.9 | 0.63 |
| Consistency (MPa) | SNV | 3 | 41.9 | 0.22 | 45.3 | 0.12 | SNV | 2 | 44.5 | 0.14 | 48.3 | 0.03 |
| | MSC | 3 | 42.0 | 0.22 | 45.9 | 0.08 | MSC | 4 | 41.6 | 0.25 | 47.5 | 0.07 |
| | d1 | 3 | 40.2 | 0.28 | 44.6 | 0.15 | d1 | 1 | 44.2 | 0.15 | 48.6 | 0.05 |
| | d2 | 2 | 40.3 | 0.28 | 44.1 | 0.17 | d2 | 1 | 45.0 | 0.18 | 48.1 | 0.01 |

SMP, slip melting point; MP85, melting point at 85% melted crystals; MP90, melting point at 90% melted crystals; MP95, melting point at 95% melted crystals; SNV, Standard Normal Variate; MSC, Multiplicative Scatter Correction; d1, first derivative; d2, second derivative; LVs, latent variables; RMSEC, root mean square error of calibration; R^2_{cal} , determination coefficient of calibration; RMSECV, root mean square error of cross-validation; R^2_{cv} , determination coefficient of cross-validation.

Table 4. Statistical parameters of PLS models constructed with selected FT-NIR and FT-IR variables for the prediction of melting and consistency properties of structured lipids.

| Response | Spectroscopy | Samples | Pretreatment | LVs | RMSEC | R^2_{cal} | RMSECV | R^2_{cv} |
|-------------------|--------------|---------|--------------|-----|-------|-------------|--------|------------|
| SMP (°C) | FT-NIR | melted | d2 | 8 | 1.5 | 0.88 | 2.03 | 0.79 |
| | FT-NIR | solid | d1 | 5 | 1.3 | 0.91 | 1.68 | 0.85 |
| | FT-IR | melted | d2 | 4 | 1.9 | 0.81 | 2.09 | 0.78 |
| | FT-IR | solid | d2 | 8 | 1.4 | 0.90 | 1.85 | 0.83 |
| MP85 (°C) | FT-NIR | melted | d2 | 9 | 2.9 | 0.87 | 3.87 | 0.78 |
| | FT-NIR | solid | SNV | 8 | 2.6 | 0.89 | 3.19 | 0.84 |
| | FT-IR | melted | d1 | 4 | 3.8 | 0.77 | 4.19 | 0.72 |
| | FT-IR | solid | d1 | 10 | 3.1 | 0.85 | 3.80 | 0.78 |
| MP90 (°C) | FT-NIR | melted | d2 | 6 | 2.7 | 0.85 | 3.51 | 0.76 |
| | FT-NIR | solid | d1 | 4 | 2.5 | 0.87 | 2.82 | 0.85 |
| | FT-IR | melted | d1 | 3 | 3.8 | 0.71 | 4.08 | 0.67 |
| | FT-IR | solid | d1 | 5 | 3.7 | 0.72 | 4.16 | 0.66 |
| MP95 (°C) | FT-NIR | melted | d1 | 8 | 2.5 | 0.84 | 3.07 | 0.76 |
| | FT-NIR | solid | SNV | 7 | 2.4 | 0.86 | 2.83 | 0.80 |
| | FT-IR | melted | SNV | 7 | 2.3 | 0.86 | 2.78 | 0.81 |
| | FT-IR | solid | d1 | 4 | 3.6 | 0.66 | 3.80 | 0.63 |
| Consistency (MPa) | FT-NIR | melted | d1 | 10 | 14.9 | 0.90 | 23.63 | 0.75 |
| | FT-NIR | solid | MSC | 9 | 11.7 | 0.94 | 13.97 | 0.91 |

SMP, slip melting point; MP85, melting point at 85% melted crystals; MP90, melting point at 90% melted crystals; MP95, melting point at 95% melted crystals; SNV, Standard Normal Variate; MSC, Multiplicative Scatter Correction; d1, first derivative; d2, second derivative; LVs, latent variables; RMSEC, root mean square error of calibration; R^2_{cal} , determination coefficient of calibration; RMSECV, root mean square error of cross-validation; R^2_{cv} , determination coefficient of cross-validation.

Fig. 1

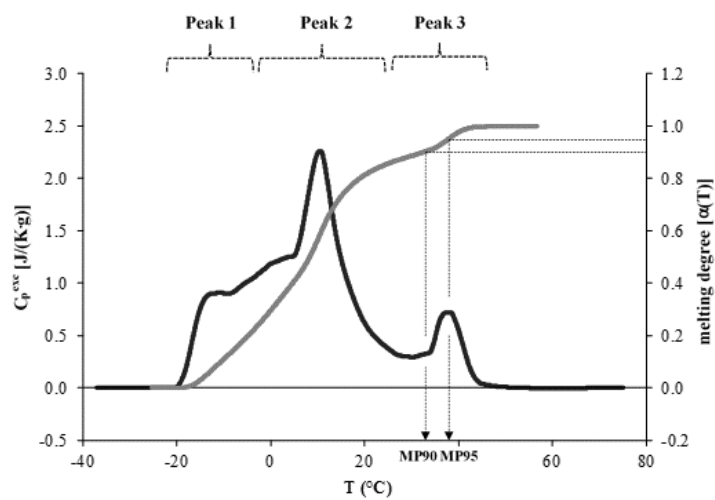


Fig. 1. Color version for online only

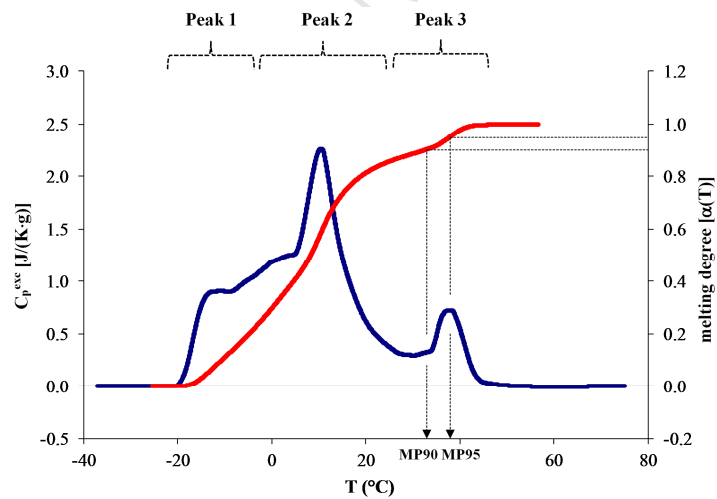


Fig. 2.

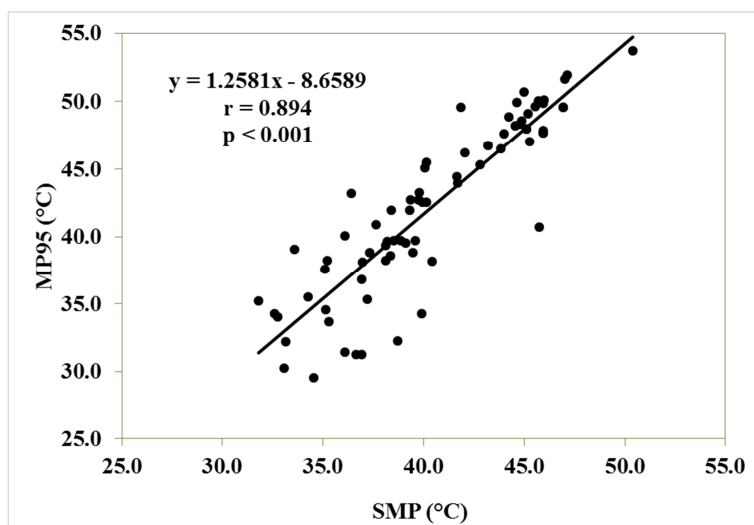


Fig. 2. Color version for online only

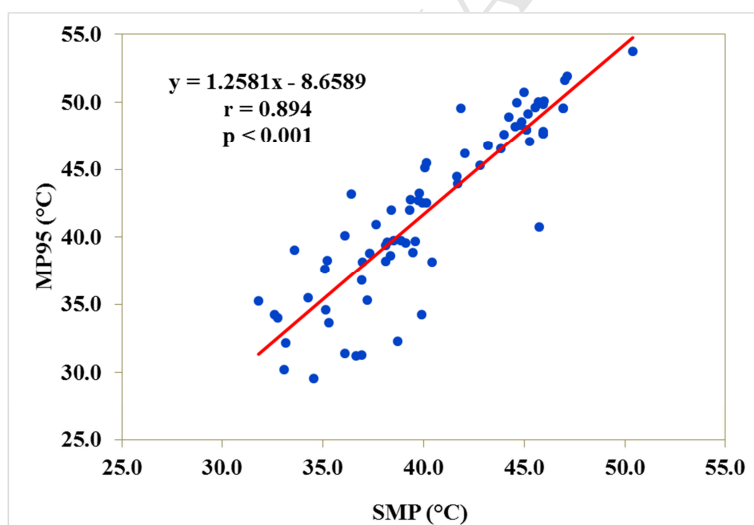


Fig. 3

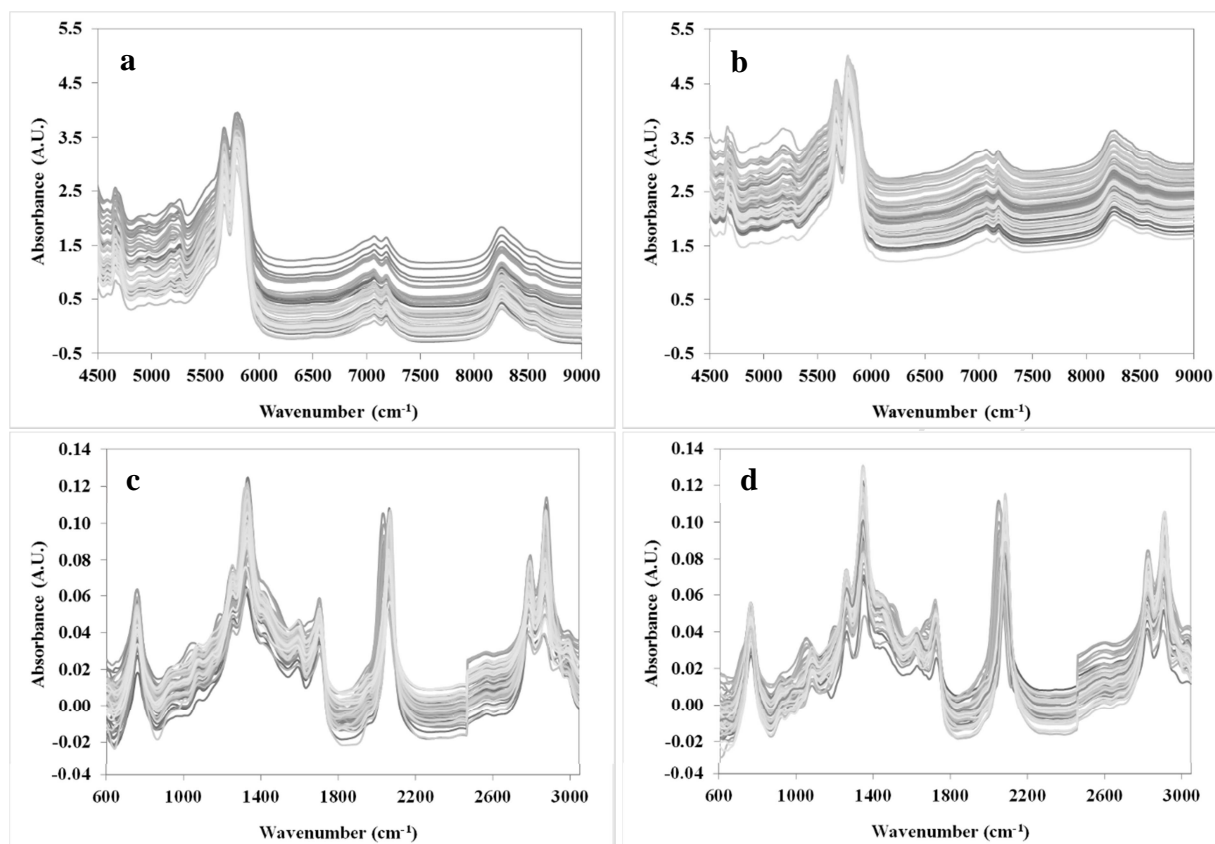
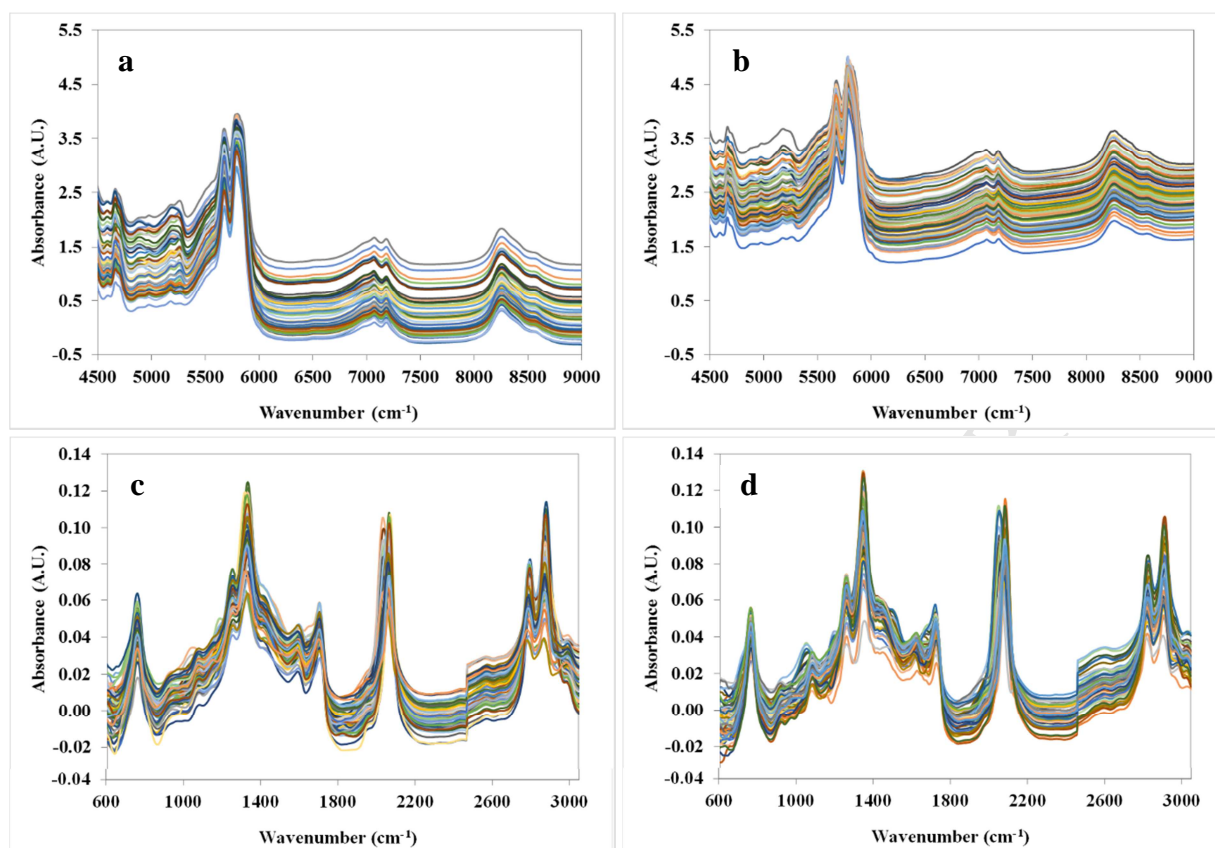


Fig. 3. Color version for online only

Highlights

- Chemical and enzymatical interesterification of tallow with three vegetable oils.
- Determination of slip melting point, melting points and consistency of structured fats.
- Collection of FT-IR and FT-NIR spectra on melted and solid samples.
- Good potential of IR spectroscopy in the prediction of fat physical properties.